Available online at www.sciencedirect.com

ScienceDirect

journal homepage: http://www.elsevier.com/locate/jab

Original Research Article

Antitumoral activity of novel 1,4-naphthoquinone derivative involves L-type calcium channel activation in human colorectal cancer cell line

Juan Carlos Ramos Gonçalves [a,b,*], *Tangbadioa Herve Coulidiati* [a], *André Luís Monteiro* [a], *Laís Campos Teixeira de Carvalho-Gonçalves* [a], *Wagner de Oliveira Valença* [c], *Ronaldo Nascimento de Oliveira* [c], *Celso de Amorim Câmara* [c], *Demetrius Antônio Machado de Araújo* [a]

[a] *Department of Biotechnology, Federal University of Paraiba, João Pessoa, Brazil*
[b] *Department of Biochemistry and Pharmacology, Federal University of Piauí, Teresina, Brazil*
[c] *Department of Molecular Sciences, Rural Federal University of Pernambuco, Recife, Brazil*

ARTICLE INFO

Article history:
Received 14 January 2016
Received in revised form
9 March 2016
Accepted 23 March 2016
Available online 7 April 2016

Keywords:
Natural products
Pharmacology
Cytotoxicity
Ion channels
HT-29
Flow cytometry
Calcium imaging

ABSTRACT

Colorectal cancer (CRC) is an important public health problem estimated as the third most commonly diagnosed cancer worldwide. Naphthoquinones are compounds present in different families of plants and interesting for medicinal chemistry due to their activities as potent inhibitors of human cancer growth. In this way, our study aimed to evaluate the cytotoxicity and selectiveness of four 2,3-triazole-1,4-naphthoquinone derivatives (N1–N4) towards the CRC cell line HT-29 and normal human cells. MTT assay showed that N1, N2, N3 and N4 elicited distinct cytotoxic potency, exhibiting EC_{50} values of 40.6 ± 1.0, 100.1 ± 1.0, 241.9 ± 1.2 and 101.9 ± 1.1, respectively. Later, flow cytometry in HT-29 cells loaded with propidium iodide (5 μM), indicated the ability of N4 (0.5–50 μM) to induce cell membrane damage. Additionally, calcium imaging experiments were conducted in HT-29 cells loaded with 5 μM Fluo-3/AM to assess intracellular Ca^{2+} (iCa^{2+}). Our data demonstrated that N4 induces a fast and strong increase of iCa^{2+} in HT-29 cells, mediated by voltage-gated L-type Ca^{2+} channels activation. In conclusion, our study reported on the cytotoxicity and selectiveness of 1,2,3-triazol substituted 1,4-naphthoquinones towards the HT-29 CRC cell line. Furthermore, we have demonstrated the participation of voltage-gated L-type Ca^{2+} channels in the N4 mechanism.

* *Corresponding author at*: Department of Biochemistry and Pharmacology, Federal University of Piauí, 64049-550 Teresina, Brazil. Tel.: +55 83 3215 5631.
E-mail address: goncalvesjcr@ufpi.edu.br (J.C.R. Gonçalves).
http://dx.doi.org/10.1016/j.jab.2016.03.002
1214-021X/

Introduction

Colorectal cancer (CRC) is an important public health problem, estimated as the third most commonly diagnosed cancer in males and the second in females worldwide, with over 1.2 million new cases and 608,700 deaths per year (Jemal et al., 2011, 2013; Pitule et al., 2013). Cancer statistics estimated that over 49,700 people in the United States would have died of CRC by the end of 2015 (Siegel et al., 2015). Even though the pharmacological remedies against cancer have improved significantly in the last twenty years, there remains the need to identify novel molecules to fight CRC.

Collective studies have shown that ion channels, the specialized membrane proteins that conduct ion fluxes, are involved in the development of many diseases including cancer (Li and Xiong, 2011). For example, the L-type calcium channel subunit, Ca_v 1.2, was found in CRC cells. Ca_v 1.2 expression increases with the differentiation of colon cells to cancer cells (Wang et al., 2000). The intracellular calcium (iCa^{2+}) ion is an important signaling factor that modulates numerous cellular processes in cancer (Clapham, 2007; Morgado et al., 2008). Ca^{2+} permeable channels, such as stored-operated calcium channels, transient receptor potential channels (TRP), and the calcium release activated channel protein 1 are involved in the iCa^{2+} homeostasis. Remodeling or deregulation of iCa^{2+} homeostasis in cancer cells causes changes in cancer progression (Parkash and Asotra, 2010). Zawadzki et al. (2008) have demonstrated that L-type calcium channels mediate calcium influx and apoptosis in human colon cancer cells that can be inhibited by verapamil a specific L-type calcium channel blocker. Thus, the identification of molecules that can activate this channel type is of great interest in CRC treatment.

Naphthoquinones are compounds present in different families of plants and considered privileged structures in medicinal chemistry due to their biological activities and structural properties (Castro et al., 2011; Padhye et al., 2012). In fact, the 1,4-naphthoquinone nucleus has become attractive as a potent inhibitor of human cancer growth and has been suggested for use in cancer therapy (Kayashima et al., 2009; Wellington, 2015). On the other hand, 1,2,3-triazoles have occupied an important role in medicinal chemistry since their facilitated synthesis by click chemistry and its attractive features (Kolb and Sharpless, 2009). They also have numerous biological activities: antifungal, antibacterial (Wang et al., 2010), anti-inflammatory (Simone et al., 2011) and anti-HIV (Giffin et al., 2008).

Inspired by the biological importance of 1,2,3-triazoles and 1,4-naphthoquinones and our recent results on the field of anticancer agents (da Cruz et al., 2014; Coulidiati et al., 2015), in this study, we relate the cytotoxicity effect of novel 1,2,3-triazole-1,4-naphthoquinone derivatives towards the human CRC cell line. In addition, we evaluate the involvement of voltage-gated calcium channels in the cytotoxic mechanisms.

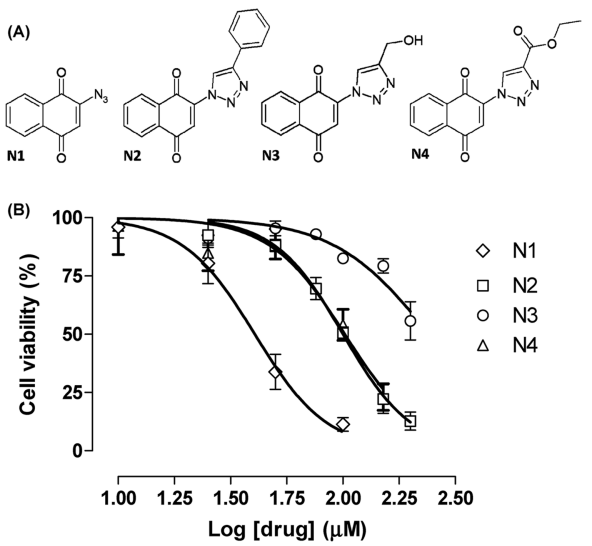

Fig. 1 – Cytotoxicity of 1,4-naphtoquinone derivatives (N1–N4) in HT-29 cells. (A) Chemical structure of the N1, N2, N3 and N4 derivatives. (B) Concentration–response curves of HT-29 colon adenocarcinoma cells incubated for 24 h with the 1,4-naphtoquinone derivatives (0.1–200 μM). Cell viability and oxidoreductase profile were determined by the MTT assay and data are displayed as mean ± SEM, obtained from at least three independent experiments in triplicate.

Materials and methods

Drugs

The 1,4-naphthoquinone derivatives ((N1, N2, N3 or N4), Fig. 1A) were synthesized at the Laboratory for Synthesis of Bioactive Compounds (UFRPE, Brazil) as previously reported (Nascimento et al., 2011).

Chemicals

RPMI-1640, propidium iodide (PI), Fluo-3 A/M, streptomycin, penicillin, etoposide were from Sigma-Aldrich (USA); 3-(4,5-dimethylthiazol-2-yl)-2,5-diphenyltetrazolium bromide (MTT), dimethylsulfoxide (DMSO), ethylenediamine tetraacetic acid (EDTA) were from Amresco (USA); foetal bovine serum (FBS) was purchased from Cripion (Brazil); ficoll-hypaque was purchased from GE Healthcare (Sweden).

Cell culture

Human colon adenocarcinoma cell line (HT-29) was acquired from Banco de Células do Rio de Janeiro (BCRJ, Brazil) and cultured in a DMEM (Himedia, India) medium supplemented with 10% FBS, 100 IU/mL penicillin, 100 mg/mL streptomycin and placed in humidified air at 37 °C with 5% CO_2 atmosphere. Normal peripheral blood mononuclear cells (PBMC) were isolated from healthy donors using Ficoll-Hypaque (Coulidiati et al., 2015), in agreement with the Committee of Ethics in Research with Humans (CEP/HULW/UFPB, Brazil), protocol #655/10-318119.

Cytotoxicity assays

The oxidoreductase profile was assessed when stock solutions of each tested compound (N1, N2, N3 or N4) were prepared in DMSO at a final concentration of 20 mM and further diluted to the desired concentrations immediately before the experiments. The total amount of DMSO in the test solutions did not exceed 0.1%. The viability of HT-29 was determined using a MTT assay, as previously described (Mosmann, 1983). Briefly, 5×10^4 cells were seeded in 96-well plates and incubated with the tested compounds (N1, N2, N3 or N4) at concentrations ranging from 0.1 to 200 μM, for 24 h in an atmosphere of 37 °C and 5% CO_2. Etoposide (ETO) 50 μM was used as the positive control. Afterward, MTT (5 mg/mL) was added in each well and incubated for an additional 3 h under the same conditions as described above. Formazan was dissolved in a SDS/HCl solution and the optical density was recorded in a spectrophotometer at 570 nm.

Plasma membrane integrity was evaluated by propidium iodide (PI). In brief, 24-well Plates 5×10^5 cells were seeded in 96-well plates and incubated with the tested compounds (N1, N2, N3 or N4) in concentrations ranging from 0.1 to 200 μM, for 24 h in a 37 °C and 5% CO_2 atmosphere. ETO 50 μM was used as the positive control. Subsequently, cells were centrifuged and then washed with PBS. The pellet was resuspended in a PI solution (5 μM), diluted in PBS and then analyzed by flow cytometry (CellQuest Pro, BD, US) to determine cell membrane damage.

Calcium imaging

The cytosolic calcium levels ($_iCa^{2+}$) in HT-29 cells were monitored by marking these cells with Fluo-3/AM and imaged in a CCD-coupled epifluorescence microscopy (ZEISS, Germany), as previously described (Gonçalves et al., 2013). Before the experiments, cells (3×10^4/well) were incubated with 5 μM Fluo-3/AM for 30 min. After this period, the cells were carefully washed three times in a free Ca^{2+}/Mg^{2+} PBS solution for an additional 30 min and imaged with a 510 nm filter. Only the viable HT-29 cells were selected and analyzed by software (AxioVision, ZEISS, Germany). The calcium-mediated relative fluorescence was quantified for each selected cell as regions of interest (ROIs) by built-in software (AxioVision, Zeiss, Germany), and then normalized as F_1/F_0, were F_1 was the maximal fluorescence emitted and F_0 was the basal fluorescence level obtained before drug incubation. Maximum and minimum fluorescence in all cells was assessed using ionomycin (IONO, 5 μM) and EGTA (20 mM), respectively, after each experiment. Data are representative for three independent experiments with at least 20 cells each, observing four different fields per plate.

Statistical analysis

Statistical difference was assessed by one-way analysis of variance (ANOVA) followed by Dunnett's or Tukey's tests at the significance level $2\alpha = 0.05$. EC_{50} values were acquired by plotting normalized data to the Hill equation: $f = Min + (Max - Min)/(1 + (IC_{50}/[\text{drug}]n))$, where, *Max* and *Min* represent the maximum and minimum values, respectively; EC_{50} is the half-maximal effective concentration of the drug tested and *n* is the Hill coefficient (Graphpad Prism, US).

Results

Four different 1,4-naphotoquinone derivatives were selected (Fig. 1A) and their cytotoxicity against HT-29 cells determined. As we observed using the MTT assay, N1, N2, N3 and N4 elicited distinct cytotoxic potential, exhibiting EC_{50} of 40.6 ± 1.0, 100.1 ± 1.0, 241.9 ± 1.2 and 101.9 ± 1.1, respectively (Fig. 1B). Additionally, N2, N3 and N4 did not induce any cytotoxicity in PBMC (data not shown).

We performed flow cytometry experiments in order to investigate the effects of N4 (0.5–50 μM) in the HT-29 membrane viability test, by staining these cells with PI (see *Methods* section). Our results demonstrated that N4 induces membrane damage in tumor cells, decreasing cell viability from 91.43 ± 2.9% (control) to 93.1 ± 0.9; 35.7 ± 12.1 and 5.3 ± 5.2 when incubated in a solution with 0.5, 5.0 and 50 μM of N4 for 24 h, respectively (Fig. 2A). Vehicle alone (DMEM and DMSO 0.1%) did not induce any significant alteration on membrane integrity, while etoposide (50 μM) decreased the

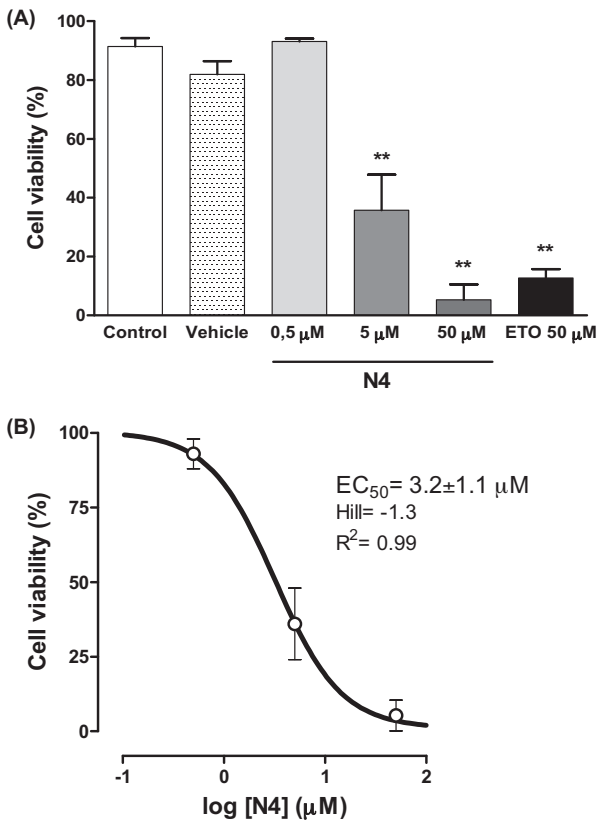

Fig. 2 – Assessment of HT-29 membrane viability. (A) HT-29 cells were submitted to 24 h-treatment with N4 (0.5–50 μM), Etoposide (ETO, 50 μM) or vehicle. (B) Concentration–response curve of HT-29 cells incubated with N4 (0.5–50 μM). Data are reported as mean ± SEM obtained from at least three independent experiments in triplicate. ANOVA: Dunnet test, *statistically significant as compared with the control.

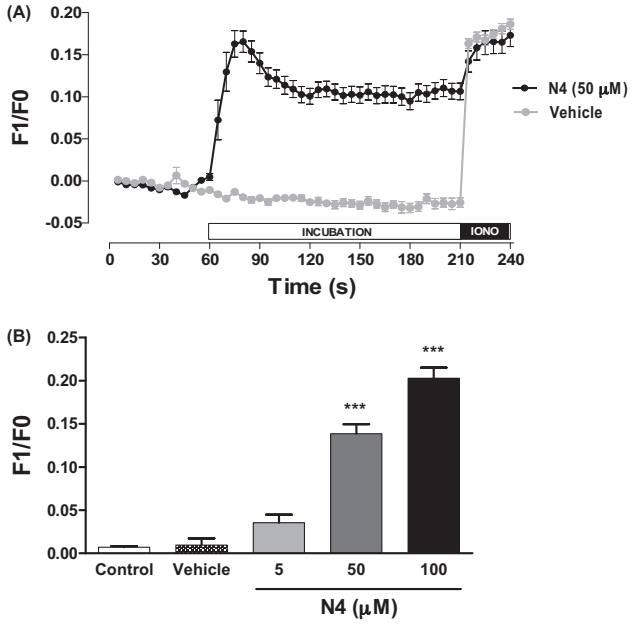

Fig. 3 – Calcium imaging assay in HT-29 cells. (A) Representative curves obtained during Calcium imaging experiments performed in HT-29 cells loaded with Fluo3 A/M and later incubated with 50 μM of N4 derivative, vehicle alone (DMSO 0.1% in PBS) and ionomycin (IONO, 5 μM). (B) Relative fluorescence (F_1/F_0) mediated by a Ca2+ intracellular increase quantified in HT-29 cells treated with N4 (5–100 μM) and vehicle alone. Data are displayed as mean ± SEM, representative of three independent experiments with at least 20 cells each, observed into four different fields per plate. ANOVA: Dunnet test, *statistically significant as compared with the control.

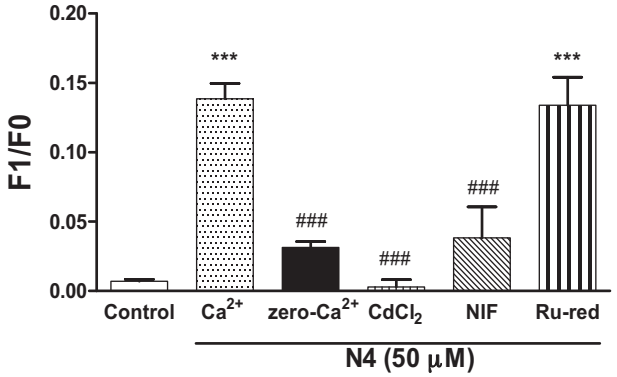

Fig. 4 – L-type calcium channel involvement in N4 mechanism. Evaluation of N4-induced Ca^{2+} pathway in HT-29 cells pre-incubated with zero-Ca^{2+} bath; $CdCl_2$ (300 μM); nifedipine (NIF, 10 μM) or ruthenium red (Ru-red, 5 μM). The relative fluorescences (F_1/F_0) are displayed as mean ± SEM from three independent experiments in triplicate. ANOVA: Tukey test, *statistically significant as compared with the control, #statistically significant as compared with the Ca^{2+} group.

viability to 12.7 ± 3.0 from control (Fig. 2A). In fact, in the flow cytometry analysis, N4 exhibited EC_{50} of 3.2 ± 1.1 μM (hill = −1.3; $R^2 = 0.99$) in a concentration dependent manner (Fig. 2B).

Calcium imaging experiments demonstrated that N4 was able to increase $_i Ca^{2+}$ in HT-29 cells at 50 μM concentration, reaching its maximum F_1/F_0 with 20 s incubation (Fig. 3A). When cells were incubated with the vehicle alone (DMSO 0.1% in PBS), no alteration in relative fluorescence was observed from basal levels (Fig. 3A). A concentration-dependent manner was observed as N4 increased F_1/F_0 from $0.7 \pm 0.1 \times 10^{-2}$ (basal) to $3.5 \pm 0.9 \times 10^{-2}$; $13.8 \pm 1.1 \times 10^{-2}$ and $20.3 \pm 1.2 \times 10^{-2}$ when HT-29 cells were incubated with 5, 50 and 100 μM, respectively (Fig. 3B).

Additionally, we evaluated the pathway of intracellular calcium increase promoted by N4 in HT-29 cells. For this, calcium imaging experiments were performed as described above. We then changed the protocol, performing the Ca^{2+} imaging experiments again using a zero-Ca^{2+} bath, or previously incubating the cells with calcium channel blockers like $CdCl_2$ (300 μM) for nonselective voltage-gated calcium channels, nifedipine (NIF, 10 μM) a selective L-type calcium channel drug and Ruthenium red (Ru-red) a nonselective TRP channel blocker at 5 μM concentration. Our data showed a calcium-mediated influx by N4 (50 μM) of about $13.9 \pm 1.1 \times 10^{-2}$ that was reduced to $3.1 \pm 0.4 \times 10^{-2}$, when the HT-29 cells were bathed with a zero-Ca^{2+} solution (Fig. 4). Relative fluorescence (F_1/F_0) was practically eliminated by $CdCl_2$ ($0.3 \pm 0.5 \times 10^{-2}$) and nifedipine ($3.8 \pm 2.2 \times 10^{-2}$). Furthermore, Ru-red was unable to block N4 effects (Fig. 4).

Discussion

The triazole nucleus is present as an important moiety in an array of drug categories: anti-microbial, anti-inflammatory, analgesic, anti-peptic, anti-viral, anti-neoplastic, anti-tubercular, anti-parkinsons, anti-diabetic, and anti-depressant, for example. The broad and potent activity of triazoles and their derivatives have made them pharmacologically significant scaffolds (Dar et al., 2015). Our study reports on the cytotoxicity of four distinct 1,4-naphthoquinone-substituted 1,2,3-triazoles (Fig. 1A) against normal and tumoral cells. Initially, we observed that N2 and N4 induced cytotoxicity in HT-29 cells, but with less potency than their precursor N1 (Fig. 1B). Despite its higher cytotoxicity against tumor cells, N1 was also toxic to normal PBMC; however, compounds N2 and N4 which contain phenyl and ester groups, respectively, are interesting, as a possible drug candidates. On the other hand, we have shown that an alcohol moiety, present in N3, abolishes the antitumoral effect (Fig. 1B). These data might be of great interest to the development of new tumor-targeted drug.

We have further observed that N4 cytotoxicity involves cell membrane damage in HT-29 cells in a concentration-dependent manner (EC_{50} = 3.2 ± 1.1 μM) (Fig. 2A and B). Interestingly, this effect was higher than the standard drug etoposide (Fig. 2A). In accordance with the MTT results, N4 did not induce any cytotoxic effect toward normal PBMC (data not shown). Thus, our data demonstrates the discrimination of the N4 derivative toward HT-29 cancer cells, but not normal human

cells. As we used only the HT-29 cell line, it is important to mention that our results might not be applicable to other CRC cells. Thus, further experiments are suggested to test their sensitivity and response to the same drugs used in this study.

A previous study with naphthoquinone-substituted molecules indicated the affinity of these molecules to plasma membrane phospholipids, inducing their disorganization and then leading to a non-specific cytotoxic effect (Hussein et al., 2013). In addition, different authors have reported high expression levels of calcium permeable ion channels in cancer cells like HT-29 (Zhang et al., 1997; Wang et al., 2000). In fact, L-type calcium channels are so highly expressed in HT-29 cancer cells, that their activators can selectively induce cell death (Zhang et al., 1997; Zawadzki et al., 2008).

To evaluate whether N4 acts by a non-specific cytotoxic effect on HT-29 cells or involves calcium permeable ion channels, calcium imaging experiments were conducted. Our data confirm that N4 induces a fast and strong increase of $_{i}Ca^{2+}$ in HT-29 cells in a concentration-dependent manner, while the vehicle alone did not induce any alteration (Fig. 3A and B). Our assumption is that the N4 mechanism involve an increase in calcium levels in HT-29 cells, although, the cellular via of such effect as well as the mechanism and specificity have not been demonstrated thus far. Therefore, additional experiments were conducted to evaluate the Ca^{2+} increase pathway involved during N4 activity in HT-29 cells. Our data show that this effect was later diminished when HT-29 cells were bathed in zero-Ca^{2+}, eliminating the intracellular Ca^{2+}-stored pathway in the N4 mechanism (Fig. 4). At the present, we might suggest that N4 was possibly promoting an ionophore-like effect or activating permeant Ca^{2+} channels through the plasma membrane. To confirm this, we pre-incubated HT-29 cells with non-selective drugs like $CdCl_2$ and Ru-red to assess the participation of voltage-gated calcium channels or TRP channels, respectively. Our results indicated the involvement of voltage-gated L-type Ca^{2+} channels during activity of the N4 mechanism, since its effects were completely nullified by $CdCl_2$ and later by nifedipine, a selective drug (Fig. 4).

As reported before, L-type Ca^{2+} channels are highly expressed in HT-29 and other cancer cell lines (Zhang et al., 1997; Zawadzki et al., 2008). Disregarding the excitable normal cells and slight exceptions (Clapham, 2007), this kind of density difference between normal and tumoral cells leads to a consideration of the L-type calcium channels as valuable targets for cancer therapy (Parkash and Asotra, 2010; Li and Xiong, 2011). Therefore, our findings might contribute to the use of N4 and derivatives in the future as an alternative to clinical treatment of patients diagnosed with CRC. Nevertheless, more study is necessary to demonstrate the clinical efficacy of the N4 compound.

Conclusion

Our study reported on the cytotoxicity and selectiveness of 1,2,3-triazol substituted 1,4-naphthoquinones towards the HT-29 CRC cell line. Furthermore, we have demonstrated the participation of voltage-gated L-type Ca^{2+} channels during the activity of the N4 derivative mechanism.

Conflicts of interest

The authors declare no conflicts of interest to disclose.

Acknowledgements

The authors are grateful to CNPq, CAPES and FACEPE-PRONEM for providing financial support.

REFERENCES

Castro, S.L., Batista, D.G., Batista, M.M., Batista, W., Daliry, A., de Souza, E.M., Menna-Barreto, R.F., Oliveira, G.M., Salomão, K., Silva, C.F., Silva, P.B., Soeiro, M.N., 2011. Experimental chemotherapy for changes disease: a morphological, biochemical, and proteomic overview of potential Trypanosoma cruzi targets of amidines derivatives and naphthoquinones. Mol. Biol. Int. 2011, 1–13.

Clapham, D.E., 2007. Calcium signaling. Cell 131, 1047–1058.

Coulidiati, T.H., Dantas, B.B., Faheina-Martins, G.V., Gonçalves, J. C., do Nascimento, W.S., de Oliveira, R.N., Camara, C.A., Oliveira, E.J., Lara, A., Gomes, E.R., Araújo, D.A., 2015. Distinct effects of novel naphthoquinone-based triazoles in human leukaemic cell lines. J. Pharm. Pharmacol. 67, 1682–1995.

da Cruz, E.H., Hussene, C.M., Dias, G.G., Diogo, E.B., de Melo, I.M., Rodrigues, B.L., da Silva, M.G., Valença, W.O., Camara, C.A., de Oliveira, R.N., de Paiva, Y.G., Goulart, M.O., Cavalcanti, B. C., Pessoa, C., da Silva Júnior, E.M., 2014. 1,2,3-Triazole-, arylamino- and thio-substituted 1,4-naphthoquinones: potent antitumor activity, electrochemical aspects, and bioisosteric replacement of C-ring-modified lapachones. Bioorg. Med. Chem. 22, 1608–1619.

Dar, M.A., Shrivastava, S., Iqbal, P.F., 2015. Click chemistry and anticancer properties of 1,2,3-triazoles. World J. Pharm. Res. 4, 1949–1975.

Giffin, M.J., Heaslet, H., Brik, A., Lin, Y.C., Cauvi, G., Wong, C.H., McRee, D.E., Elder, J.H., Stout, C.D., Torbett, B.E., 2008. A copper(I)-catalyzed 1,2,3-triazole azidealkyne click compound is a potent inhibitor of a multidrug-resistant HIV-1 protease variant. J. Med. Chem. 51, 6263–6270.

Gonçalves, J.C., Silveira, A.L., de Souza, H.D., Nery, A.A., Prado, V. F., Prado, M.A., Ulrich, H., Araújo, D.A., 2013. The monoterpene (−)-carvone: a novel agonist of TRPV1 channels. Cytom. Part A 83, 212–219.

Hussein, N., Lopes, C.C., Pernambuco Filho, P.C., Carneiro, B.R., Caseli, L., 2013. Surface chemistry and spectroscopy studies on 1,4-naphthoquinone in cell membrane models using Langmuir monolayers. J. Colloid Interface Sci. 402, 300–306.

Jemal, A., Bray, F., Center, M.M., Ferlay, J., Ward, E., Forman, D., 2011. Global cancer statistics. CA Cancer J. Clin. 61, 69–90.

Jemal, A., Simard, E.P., Dorell, C., Noone, A.-M., Markowitz, L.E., Kohler, B., Eheman, C., Saraiya, M., Bandi, P., Saslow, D., Cronin, K.A., Watson, M., Schiffman, M., Henley, S.J., Schymura, M.J., Anderson, R.N., Yankey, D., Edwards, B.K., 2013. Annual Report to the Nation on the Status of Cancer, 1975-2009, featuring the burden and trends in human papillomavirus (HPV)-associated cancers and HPV vaccination coverage levels. J. Natl. Cancer Inst. 105, 175.

Kayashima, T., Mori, M., Yoshida, H., 2009. 1,4-Naphthoquinone is a potent inhibitor of human cancer growth and angiogenesis. Cancer Lett. 278, 34–40.

Kolb, H.C., Sharpless, K.B., 2009. The growing impact of click chemistry on drug discovery. Drug Discov. Today 8, 1128–1137.

Li, M., Xiong, Z.-G., 2011. Ion channels as targets for cancer therapy. Int. J. Physiol. Pathophysiol. Pharmacol. 3, 156–166.

Morgado, S., Granados, M.P., Bejarano, I., López, J.J., Salido, G.M., González, A., Pariente, J.A., 2008. Role of intracellular calcium on hydrogen peroxide-induced apoptosis in rat pancreatic acinar AR42J cells. J. Appl. Biomed. 6, 211–224.

Mosmann, T., 1983. Rapid colorimetric assay for cellular growth and survival: application to proliferation and cytotoxicity assays. J. Immunol. Methods 65, 55–63.

Nascimento, W.S., Camara, C.A., Oliveira, R.N., 2011. Synthesis of 2(1*H*-1,2,3-triazol-1-yl)-1,4-naphthoquinones from 2-azido-1,4-naphthoquinone and terminal alkynes. Synthesis 20, 3220–3224.

Padhye, S., Dandawate, P., Yusufi, M., Ahmad, A., Sarkar, F.H., 2012. Perspectives on medicinal properties of plumbagin and its analogs. Med. Res. Rev. 32, 1131–1158.

Parkash, J., Asotra, K., 2010. Calcium wave signaling in cancer cells. Life Sci. 87, 587–595.

Pitule, P., Cedikova, M., Treska, V., Kralickova, M., Liska, V., 2013. Assessing colorectal cancer heterogeneity: one step closer to tailored medicine. J. Appl. Biomed. 11, 115–129.

Siegel, R.L., Miller, K.D., Jemal, A., 2015. Cancer statistics. CA Cancer J. Clin. 65, 5.

Simone, R.D., Chini, M.G., Bruno, I., Riccio, R., Mueller, D., Werz, O., Bifulco, G., 2011. Structure-based discovery of inhibitors of microsomal prostaglandin E2 synthase-1,5-lipoxygenase and 5-lipoxygenase-activating protein: promising hits for the development of new anti-inflammatory agents. J. Med. Chem. 54, 1565–1575.

Wang, X.-T., Nagaba, Y., Cross, H.S., Wrba, F., Lin Zhang, L., Sandra, E., Guggino, S.A., 2000. The mRNA of L-type calcium channel elevated in colon cancer. Am. J. Pathol. 157, 1549–1562.

Wang, X.L., Wan, K., Zhou, C.H., 2010. Synthesis of novel sulfanilamide-derived 1,2,3-triazoles and their evaluation for antibacterial and antifungal activities. Eur. J. Med. Chem. 45, 4631–4639.

Wellington, K.W., 2015. Understanding cancer and the anticancer activities of naphthoquinones – a review. RSC Adv. 5, 20309–20338.

Zawadzki, A., Liu, Q., Wang, Y., Melander, A., Jeppsson, B., Thorlacius, H., 2008. Verapamil inhibits L-type calcium channel mediated apoptosis in human colon cancer cells. Dis. Colon Rectum 51, 1696–1702.

Zhang, L., Zhou, W., Velculescu, V.E., Kern, S.E., Hruban, R.H., Hamilton, S.R., Vogelstein, B., Kinzler, K.W., 1997. Gene expression profiles in normal and cancer cells. Science 276, 1268–1272.